THE ASTROPHYSICAL JOURNAL, 361:69–77, 1990 September 20

CHAOTIC ORBITS IN BARRED GALAXIES WITH CENTRAL MASS CONCENTRATIONS

HASHIMA HASAN
Space Telescope Science Institute
AND
COLIN NORMAN
Department of Physics and Astronomy, Johns Hopkins University; and Space Telescope Science Institute
Received 1989 November 14; accepted 1990 March 20

ABSTRACT

We study the dynamical interaction of a black hole or central mass concentration with the inner regions of a rapidly rotating barred galaxy. Stochastic regions appear as the central mass is increased. These are associated with the appearance and outward movement of an inner Linblad resonance related to an increase of central mass. The fundamental family of orbits sustaining the bar will dissolve at approximately the point where this resonance reaches the end of the bar. More elongated bars dissolve more easily and orbits closer to the center become stochastic more readily.

Subject headings: galaxies: internal motions — galaxies: structure

I. INTRODUCTION

The effect of the growth of a central mass concentration in a rapidly rotating barred galaxy on the stellar dynamics of the central regions of the parent galaxy is examined. This is an interesting problem because large mass concentrations are known to exist in the centers of elliptical galaxies such as M87 (Sargent *et al.* 1978; Dressler 1988) and nearby spirals such as M31 and M32 (Tonry 1987; Kormendy 1988; Richstone and Dressler 1988). Ultraluminous starburst galaxies such as Arp 220 are inferred to have 10^{10} $M_\odot$ or more within the central 300 pc (Scoville *et al.* 1987). The recently discovered counter-rotating cores seen in ellipticals have similar characteristics (Franx and Illingworth 1989; Jedrzejewski and Schechter 1989). Theoretical estimates of the mass fuelling rates for quasars are of order 10 $M_\odot$ yr^{-1} for $\sim 10^8$ yr. This central mass estimate of at least 10^9 $M_\odot$ can be significantly higher if the efficiency factors are lowered. Although many papers have been written on how the formation of such central mass concentrations can power AGNs and starbursts (see Rees 1984), relatively little has been done to try and understand their influence on stellar motion.

Certain features of stellar orbits in stationary or slowly rotating potentials with a small central mass concentration have been studied by other authors. Gerhard and Binney (1985) showed how a central point mass, M_h, embedded in a galactic nucleus of velocity dispersion σ, will scatter stars that enter its sphere of influence of radius $r_h \sim GM_h/\sigma^2$. Stars entering in one family of box orbits have a probability of emerging in another family of orbits. They estimated that for typical parameters the box orbits would be disrupted out to ~ 2 kpc from the center if the ratio of M_h to the core mass, $M_{\rm core}$, was $\sim 2\%$.

Norman, May, and van Albada (1985) studied the problem using self-consistent N-body models. They took a typical N-body galaxy model, put in a central mass, and watched the evolution. The most difficult task was to disentangle the necessarily poor orbit integration of the N-body code within galactocentric radius, r_h, from real secular evolution. They found significant roundening of the galaxy out to ~ 7 core radii. It is interesting to note that the overall orbit distributions were very well conserved, although there was frequent scattering between orbit families (due to both real and numerical effects) but the populations were consistent with slow secular evolution. A. May and C. A. Norman (1985, unpublished) studied orbits in a nonrotating bar system and looked at the relative areas of the surface of section populated by different orbit families as a function of the central mass. For a ratio of central to core mass of 0.1% or smaller, the orbits were the standard box orbits but as this parameter rose to between 0.1% and 10% the region was dominated by stochastic orbits. For values of $M_h/M_{\rm core} \geq 10\%$ the orbits became increasingly tubelike as is expected as the central mass begins to dominate. Lake and Norman (1983) gave a preliminary discussion of gas in very weakly dissipative Hamiltonian systems and showed how Mel'nikov's theorem implied that the gas clouds orbiting in galaxies will attempt to find the stable periodic orbits.

Udry and Pfenniger (1988) examined ellipsoidal potentials with Rood profiles and calculated the Liapunov exponents over ~ 2 Hubble times. Using the definition of the Kolmogorov entropy which is the sum of the positive Liapunov exponents they showed that the addition of a central mass concentration of order $\sim 2\%$ increases the average entropy by $\sim 80\%$ and noted that this will force the evolution away from, for example, integrable Stäckel systems. Pfenniger and De Zeeuw (1989) studied the homogeneous triaxial ellipsoids with regular boxes in the core and found they exhibited stochastic orbits when a core mass was added. They conjectured that shapes of cores may stabilize at the resonant homogeneous ellipsoids with integral frequency ratios. Miralda and Schwarzschild (1989) showed how the centrally concentrated singular logarithmic potential cannot support box orbits, merely boxlets. These can become unstable due to scattering off the central mass concentration.

Further study of this fascinating problem is almost irresistible, and in this paper we have studied the two-dimensional problem of the dynamics of a bar and black hole. In particular, we examine the onset of stochasticity and establish the point at which the central mass concentration becomes sufficiently massive to dissolve the principal family of orbits sustaining the bar. In § II we formulate the problem, in § III we give the results, and in § IV we summarize.

II. MODEL POTENTIAL AND FORMULATION

The galaxy was modeled by a two-component rotating potential to which was added a central compact object representing a black hole or central mass concentration. The model potential Ψ was chosen to have an axisymmetric core which was taken to be a Plummer sphere given by

$$\Psi_c = \frac{-GM_c}{\sqrt{(A_c^2 + R^2)}}\,, \tag{1}$$

where A_c is the scale length of the sphere, M_c, the total mass of the sphere, and G the gravitational constant. The second component of the galactic potential was modeled by an inhomogeneous prolate ellipsoid with a density distribution of the form

$$\rho = \begin{cases} \rho_0(1 - m^2)^2 & \text{if } m < 1 \\ 0 & \text{if } m > 1 \end{cases}\,, \tag{2}$$

where $m^2 = (x^2/a^2) + (y^2 + z^2)/b^2$, with $a > b$. We shall restrict ourselves to the galactic plane where $z = 0$. This potential is a reasonable representation of a bar and has been used by several authors (e.g., Teuben and Sanders 1985; Athanassoula *et al.* 1983). It has a density falling smoothly to zero, giving a continuous potential at the edge of the bar. It has the advantage that its analytic form is well defined (Perek 1962, for the oblate case; de Vaucouleurs and Freeman 1972), and is easily computed in terms of index symbols (Chandrasekhar 1969) which are functions of b/a and are constant within the spheroid while they vary with the radial distance outside the bar. Teuben and Sanders (1985) also add a halo component to their potential. We ignore this component as we are interested only in orbits which are affected by the black hole. The effect of the halo is expected to be insignificant in this region.

The central compact object was also modeled by a Plummer sphere.

$$\Psi_{bh} = \frac{-GM_{\rm bh}}{\sqrt{(A_{bh}^2 + R^2)}}\,. \tag{3}$$

The free parameters of this potential are as follows: (1) the relative mass ratio of the bar M_b/M_T, where $M_T = M_b + M_c + M_{\rm bh}$, (2) the semimajor axis of the bar a, (3) the bar axial ratio b/a, (4) the ratio of the length scale of the central component to the length of the bar A_c/a, (5) the ratio of the corotation radius to the length of the bar, R_{cr}/a, or equivalently the pattern speed Ω_p, (6) the black hole mass ratio $M_{\rm bh}/M_T$, (7) the ratio of the length scale of the black hole potential to the length of the bar $A_{\rm bh}/a$. The black hole has been softened for computer efficiency and numerical accuracy since the force at small distances is very large and very short time steps would be required in the numerical integration of the equations of motion to follow the motion accurately.

For normalization purposes it was found convenient to fix the bar semimajor axis a at 9 kpc and the total mass $M_T = 4.67 \times 10^{10}\ M_\odot$ (Teuben and Sanders 1985). For all cases studied this normalization resulted in a pattern speed $\Omega_p \sim 15$ km s^{-1} kpc so that $R_{cr}/a = 1$.

We examined the effect of the black hole on the orbits of this potential for three sets of conditions:

1. *Black hole mass was varied.* The bar parameters were fixed at $M_b/M_T = 0.3$, $b/a = 0.45$, $A_c/a = 0.5$, $A_{bh}/a = 0.05$. As the black hole mass was varied, the core mass was allowed to vary so that the total mass remained constant. The Jacobi constant was fixed so that a star could reach a maximum distance of $0.45a$.

2. *The value of b/a was varied.* The value of b/a was changed from 0.45 to 0.35, 0.25, while the following parameters were held constant at $M_b/M_T = 0.3$, $A_c/a = 0.5$, $A_{\rm bh}/a = 0.05$, $M_{\rm bh}/M_T = 0.03$. The Jacobi constant was fixed so that a star could reach a maximum distance of $0.45a$.

3. *Jacobi constant was varied.* This was done so that a star could reach a maximum distance of $0.25a$, $0.45a$, and $0.65a$. The potential parameters were fixed at $M_b/M_T = 0.3$, $b/a = 0.45$, $A_c/a = 0.5$, $A_{\rm bh}/a = 0.05$, $M_{\rm bh}/M_T = 0.03$.

We consider the motion of a star in the $x - y$ plane of a galaxy rotating with a pattern speed Ω_p. The Hamiltonian of the system (Jacobi integral) in the frame of rotation is

$$H = \tfrac{1}{2}(\dot{x}^2 + \dot{y}^2) + \Psi(x, y) - \tfrac{1}{2}\Omega_p^2(x^2 + y^2) \tag{4}$$

where $(x, y, \dot{x}, \dot{y})$ are the phase coordinates. The equations of motion have the standard form (Binney and Tremaine 1987; De Zeeuw and Merritt 1983)

$$\frac{dx}{dt} = \dot{x}\,, \tag{5}$$

$$\frac{dy}{dt} = \dot{y}\,, \tag{6}$$

$$\frac{d\dot{x}}{dt} = -2\Omega_p\dot{y} - \frac{\partial\Psi}{\partial x} + \Omega_p^2 x\,, \tag{7}$$

$$\frac{d\dot{y}}{dt} = 2\Omega_p\dot{x} - \frac{\partial\Psi}{\partial y} + \Omega_p^2 y\,. \tag{8}$$

For a particular value of the Jacobi integral, orbits were obtained by numerically integrating the equations of motion with initial conditions corresponding to the star being on the y-axis with $\dot{y} = 0$ and $\dot{x}$ computed from equation (4). A seventh to eighth order Runge-Kutta integration scheme (Fehlberg 1969, 1970) was used for the computation. Surface of section plots were made by storing the values of $(y, \dot{y})$ every time the star crossed the y-axis with a positive value of $\dot{x}$ (or equivalently, values of $(-y, -\dot{y})$ for crossings of the y-axis with negative x-velocity). As a check of numerical accuracy, in a number of test cases values of $|(J - J_0)/J|$, where J and J_0 are respectively, the values of the Jacobi constant at the starting point and the surface of section point, were computed. They came out to be typically of the order of 10^{-9} and nowhere exceeded 10^{-7}.

Before going on to examine the nature of orbits and surfaces of section, we shall outline the numerical technique employed to compute the phase space volumes discussed in later sections of this paper. Let us consider orbits with Hamiltonian values in the range $(J + \delta J, J)$ which fill a region D in the appropriate phase space surface of section [in our case (H = const, $x = 0$)]. The volume, $\delta\tau$, in phase space occupied by orbits which start in the region D is given by (Binney, Gerhard, and Hut 1985)

$$\delta\tau = \delta J \int_D T(y, \dot{y})\,dy\,d\dot{y}\,, \tag{9}$$

where $T(y, \dot{y})$ is the time required for the orbit which starts from $(0, y, \dot{x}, \dot{y})$ with Jacobi constant J to return to the surface of section ($H = J$, $x = 0$). We use this formula in our computation of phase space volumes.

The numerical integration is carried out by using the NAG library routine D01DAF which employs the method described by Patterson (1968*a*, *b*), of the optimum addition of points to Gauss quadrature formulae. The routine attempts to evaluate to specified absolute accuracy a definite integral of the form

$$I = \int_a^b \int_{\phi_1(y)}^{\phi_2(y)} f(x, y) dx\, dy \,, \tag{10}$$

where a and b are constants and ϕ_1 and ϕ_2 are functions of the variable y. In our case, the limits a and b are replaced by the limiting values of y on the phase space curve. Since the phase space that we are interested in (see § III) is symmetrical about the y-axis (in the $(y, \dot{y})$ plane), we need consider the bounding curve above the y-axis only. Thus we have $\phi_1(\dot{y}) = 0$, while $\phi_2(\dot{y})$ is determined by the particular phase space area under consideration. In the case of the total phase space $\phi_2(\dot{y})$ is just the "zero velocity" curve defined by the equation

$$\dot{y} = \sqrt{\{2[J - \Psi(0, y)] + \Omega_p^2 y^2\}} \,. \tag{11}$$

The other curves in the $(y, \dot{y})$ plane that we shall be interested in are well-behaved univalued invariant curves symmetric in $(\dot{y}, -\dot{y})$. As before we consider the bounding curve above the y-axis only so that $\phi_1(\dot{y}) = 0$, and $\phi_2(\dot{y})$ is given numerically by the phase space points (or consequents) defining the invariant curves. The points are first ordered so that they follow one another along a smooth curve. Interpolation between the points is done by a cubic spline with end point conditions corresponding to the "not-a-knot" condition (De Boor 1978) which requires that the third derivative of the spline be continuous at the second and penultimate knots. The interpolation routine ICSCCU from the ISML library was used.

Finally, it is instructive to look at three-dimensional plots of $T(y, \dot{y})$ versus y and $\dot{y}$ values corresponding to direct orbits. We show two examples in Figure 1. The first case (Fig. 1*a*) is that of a rotating bar with no black hole. We see that T is fairly constant over the entire range considered. Some points of discontinuity are found for small values of y. An examination of the orbits at these points shows that they are partially retrograde as they develop a loop along the y-axis which causes them to return to the surface of section much faster than the orbits which are purely direct. Excluding these points of discontinuity the values of T fluctuate between roughly $+8\%$ and roughly -12% of the mean. The second case (Fig. 1*b*) is that of a rotating bar with a black hole mass 0.17 M_T. In this case there are larger fluctuations in T, between roughly $+31\%$ and roughly -33% of the mean. This is not surprising as almost all orbits in the region of phase space considered are stochastic (see § III). Binney, Gerhard, and Hut (1985) pointed out that the phase space volume is proportional to the area occupied by the orbits in the surface of section only if $T = \text{const}$. Thus while it might be a reasonable approximation to compute the area of the surface of section for the rotating bar without a black hole as a measure of the phase space volume, this can no longer be done when stochastic orbits are dominant and the full phase-space volume should be computed according to equation (9).

III. DISCUSSION OF RESULTS

a) Variation of Black Hole Mass

An examination of the surface of section (Fig. 2*a*) shows that in the absence of a black hole there is one family of direct orbits aligned with the bar, represented by the invariant curves on the right of the figure, and one family of retrograde orbits, represented by the invariant curves on the left of the figure. We shall not discuss the retrograde orbits further as they are unimportant for supporting bars. Following Athanassoula *et al.*

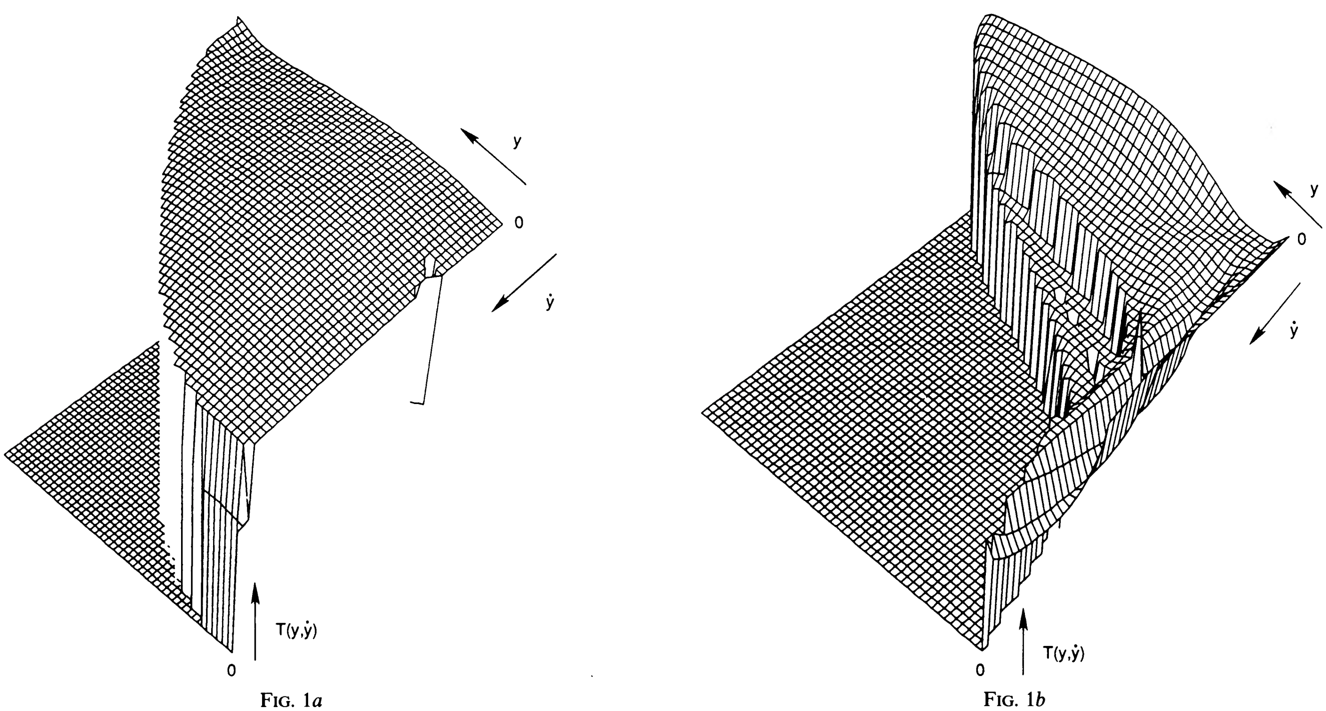

FIG. 1*a* FIG. 1*b*

FIG. 1.—Three-dimensional plot of $T(y, \dot{y})$ for a rapidly rotating bar with (*a*) no black hole and (*b*) $M_{bh}/M_T = 0.17$

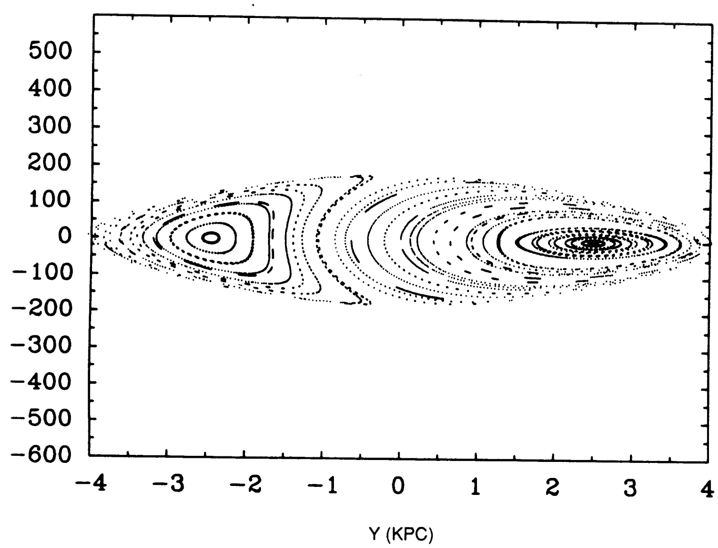

FIG. 2*a*

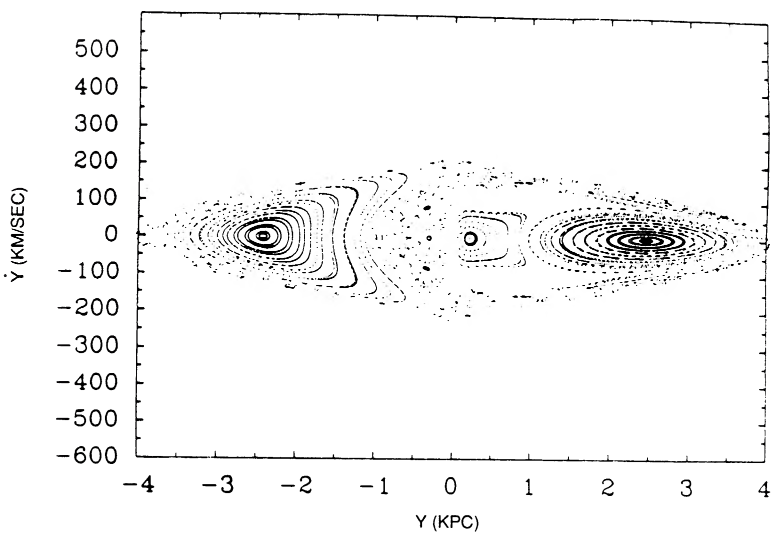

FIG. 2*b*

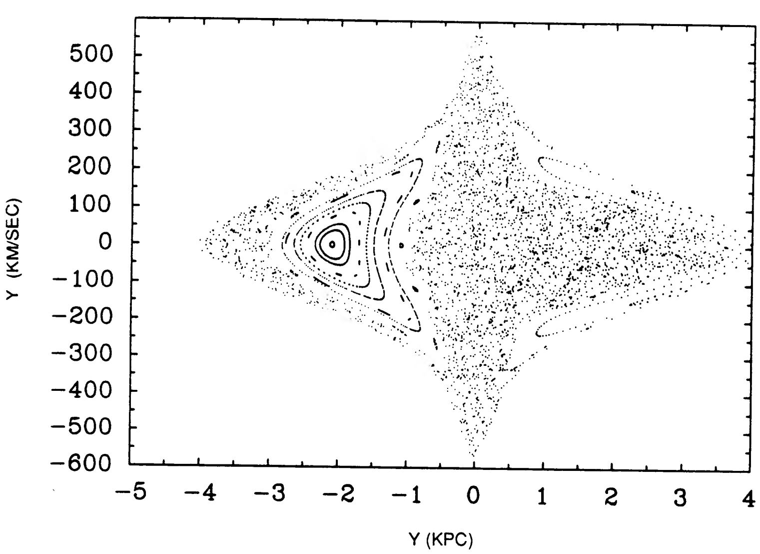

FIG. 2*c*

FIG. 2.—Surface of section plots for a rapidly rotating bar with $b/a = 0.45$, Jacobi constant corresponding to the particle reaching a maximum distance of $0.45a$ and with (*a*) no black hole, (*b*) $M_{\rm bh}/M_T = 0.01$, and (*c*) $M_{\rm bh}/M_T = 0.17$.

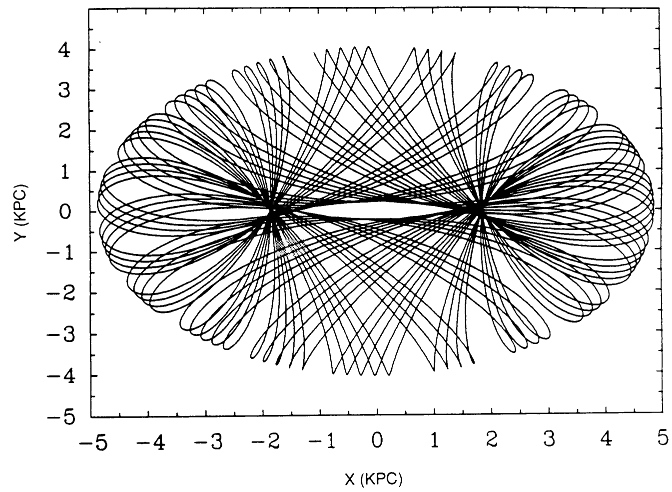

FIG. 3*a*

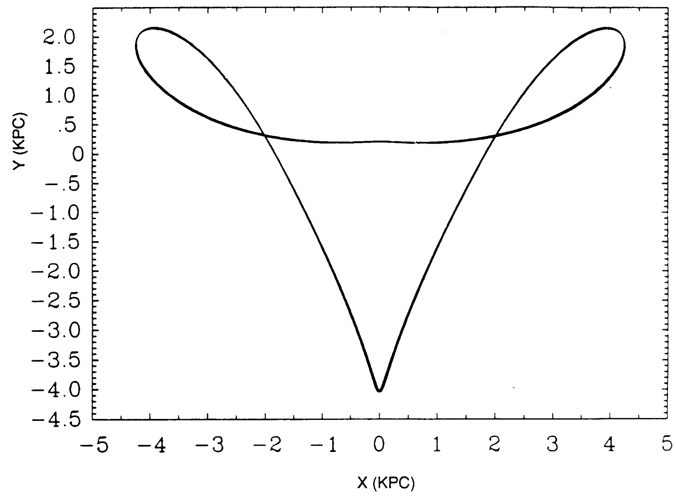

FIG. 3*b*

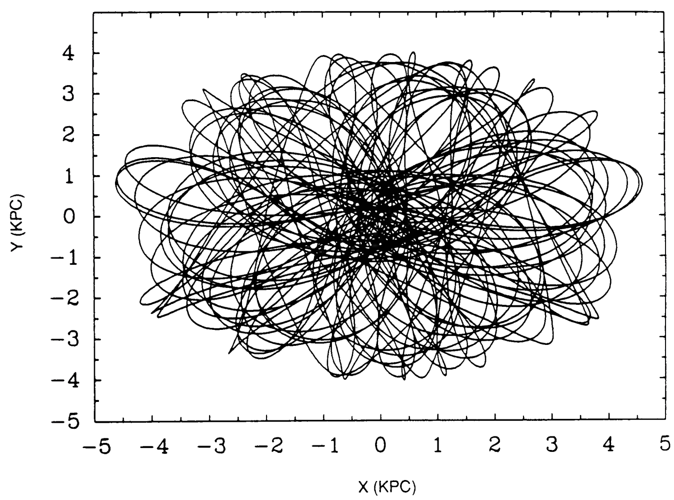

FIG. 3*c*

FIG. 3.—Evolution of an orbit starting at (0, 0.21) for a rapidly rotating bar with (*a*) no black hole, (*b*) $M_{\rm bh}/M_T = 0.01$, and (*c*) $M_{\rm bh}/M_T = 0.07$.

(1983), we shall refer to this family of direct orbits as family *B*. The orbits are all loops as is apparent from the invariant curves (IC) representing them in the surface of section. The introduction of a central black hole with $M_{\rm bh}/M_T = 0.005$ does not change the nature of the surface of section. Increasing the black hole mass ratio to 0.009 causes the appearance at small radii of a minor family of loop orbits. For $M_{\rm bh}/M_T = 0.01$ this minor orbit family leads to well-defined invariant curves in the surface of section, lying between the retrograde family and the *B* family (Fig. 2*b*). These direct orbits are anti-aligned with the bar. We shall refer to them as "looplets" in analogy with the minor family of box orbits christened as "boxlets" by Miralda *et al.* (1989). The corresponding parent periodic orbit is shown in Fig. 3*b*. The looplets persist as the black hole mass ratio is increased to 0.011, although the outermost looplet gets converted to a loop of the major orbit family. As $M_{\rm bh}/M_T$ is further increased to 0.013 all the looplets join the major orbit family *B*. Between $M_{\rm bh}/M_T = 0.013$ and 0.05 the two outermost orbits become stochastic and the corresponding invariant curves in the surface of section dissolve. As the black hole mass is increased further more orbits become stochastic until at mass ratio 0.17 all *B* family orbits have become stochastic and the bar dissolves completely. At mass ratio 0.11 we see the appearance of some orbits antialigned to the bar (*A* type of orbits) at large distances from the center. These remain as the mass ratio is increased.

The evolution of the orbit of a particle which starts off at (0, 0.21) with $\dot{y} = 0$, with increasing black hole mass is illustrated in Figure 3. An orbit of family *A* which appears at large black hole masses is shown in Figure 4.

An estimate of stochasticity was obtained by computing the percentage *P* of the phase space volume occupied by the *B* family of orbits following the method outlined in § II. In order to decide which invariant curve should be used as the boundary of the space, each curve was plotted individually on the screen and its endpoints tabulated. The curves were examined by eye, and the outermost curve that looked smooth was used. In cases where it was difficult to distinguish between the smoothness of two adjacent curves, volumes were computed for both cases and the mean taken. The results are plotted in Figure 5 versus the black hole mass ratio. Between mass ratios 0 and 0.005 the phase space occupied by *B* orbits goes from

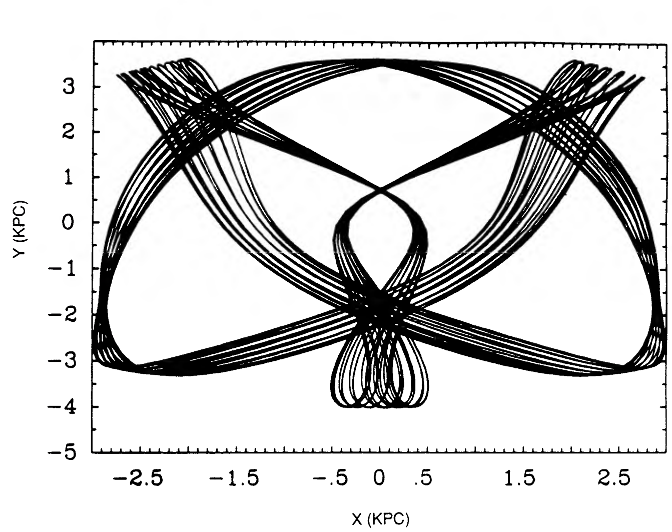

FIG. 4.—An example of a type *A* orbit appearing at large black-hole masses. This is a short time snapshot.

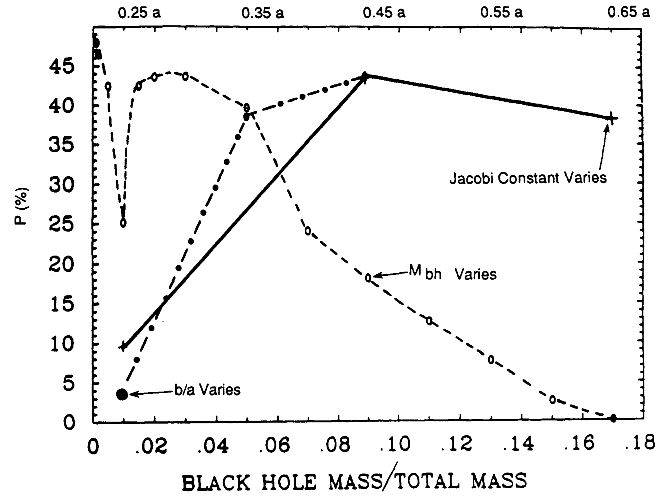

FIG. 5.—Percentage of phase space occupied by B orbits. The lines are a guide to the eye and do not represent a fit.

~48% to ~42%. For $M_{bh}/M_T = 0.01$ this percentage, P, falls to ~25% because of the appearance of the looplets. The value of P goes back to ~42% for a black hole mass ratio of 0.015 and stays around that value until $M_{bh}/M_T = 0.03$, after which it starts falling until it reaches zero for a black hole mass ratio of 0.17.

Physical insight may be gained by using the results of the epicycle theory of nearly circular orbits in an axisymmetric potential as applied to loop orbits in weak bars (Binney and Tremaine 1987). It has been shown that a self-consistent weak bar is composed primarily of orbits which are parallel to the bar and that such a bar can only be present inside corotation in regions where $\Omega_p > \Omega - \kappa/2$, where $\Omega(R)$ and $\kappa(R)$ are the circular and epicycle frequencies, respectively, of an orbit at the radial position R. A detailed study of orbits in bars by Contopoulos and Papayannopoulos (1980) also shows that for weak bars the B family of orbits lie between the outer inner Lindblad resonance (ILR), when $\Omega_p = \Omega(R_{ILR}) - \kappa(R_{ILR})/2$, and the corotation radius, when $\Omega_p = \Omega(R_{CR})$. Extending these results to the case of a rapidly rotating bar perturbed by a small central mass concentration we would qualitatively expect the region in phase space occupied by B orbits to decrease as the outer ILR moves outward. It must be kept in mind that these ideas are very approximate for this problem, and although the Lindblad resonance is not strictly defined we only use the concept to get some physical insight (see Teuben and Sanders 1985 and van Albada and Sanders 1982 for a discussion of the Lindblad resonances with reference to rapidly rotating strong bars).

Since the potential we consider here is not circular we consider the behavior of $\Omega(R)$ and $\kappa(R)$ along the x and y axes. For the Lagrangian points in a nonaxisymmetric potential they are given by (Pfenniger 1990)

$$\Omega_x^2 \equiv \Omega(x, 0) = \Psi_x(x, 0)/x \,, \tag{12}$$

$$\Omega_y^2 \equiv \Omega(0, y) = \Psi_y(0, y)/y \,, \tag{13}$$

$$\kappa_x^2 \equiv \kappa^2(x, 0) = \Psi_{xx}(x, 0) + \Psi_{yy}(x, 0) + 2\Psi_x(x, 0)/x \,, \tag{14}$$

$$\kappa_y^2 \equiv \kappa^2(0, y) = \Psi_{xx}(0, y) + \Psi_{yy}(0, y) + 2\Psi_y(0, y)/y \,. \tag{15}$$

Here $\Psi_x(x, y)$ and $\Psi_y(x, y)$ represent partial derivatives of the potential with respect to x and y, respectively, and $\Psi_{xx}(x, y)$ and $\Psi_{yy}(x, y)$ are the corresponding second derivatives. In real bars, periodic orbits are not circular, and at a given radius different transverse frequencies hold for each family. The above expressions are good for circular orbits but only approximate for elongated orbits.

An examination of the curves for $\Omega_{x(y)}$ and $\Omega_{x(y)} - \kappa_{x(y)}/2$ shows that in the absence of a black hole the pattern speed Ω_p is much higher than $\Omega - \kappa/2$ so that there are no Lindblad resonances (Fig. 6a) and all direct orbits are of the B type. The situation does not change with the introduction of a black hole of mass 0.005 M_T. However, as the mass of the black hole increases the peak in $\Omega - \kappa/2$ rises sharply (Fig. 6b) and we see the appearance of the inner Lindblad resonances (ILRs). In Table 1 we show the values of the outer ILRs along the x- and y-axis, respectively, as the black hole mass increases. The pattern speeds along x and y are computed from equations (12) and (13) at $(R_{cr}, 0)$ and $(0, R_{cr})$, respectively. The ILR along a particular axis corresponds to the radial distance along that axis when the pattern speed is equal to $\Omega - \kappa/2$. The outer ILR along the x-axis moves out from 0.8 kpc to 2.3 kpc while that

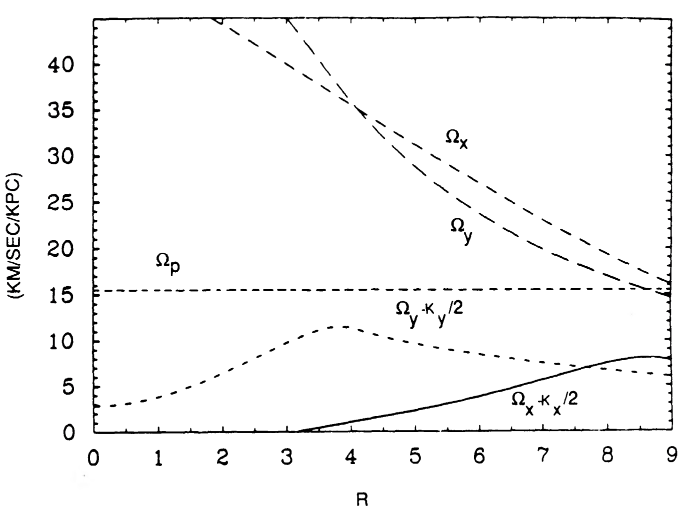

FIG. 6a

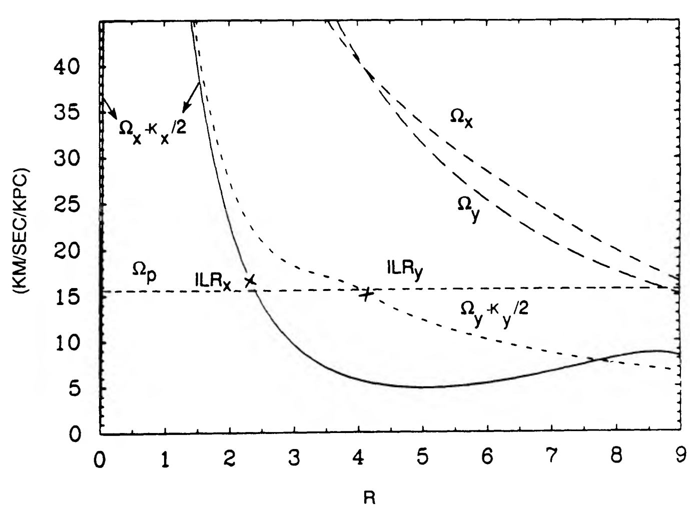

FIG. 6b

FIG. 6.—Frequency plots for (a) no black hole and (b) $M_{bh}/M_T = 0.17$. The corotation radius is 9 kpc

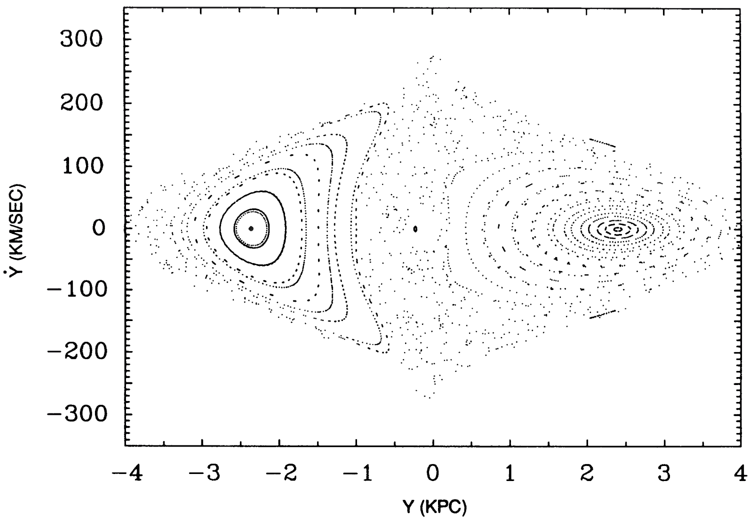

FIG. 7*a*

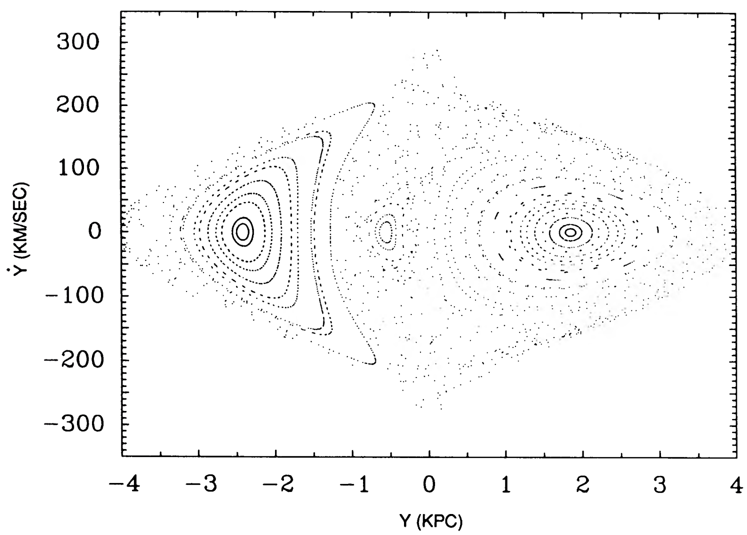

FIG. 7*b*

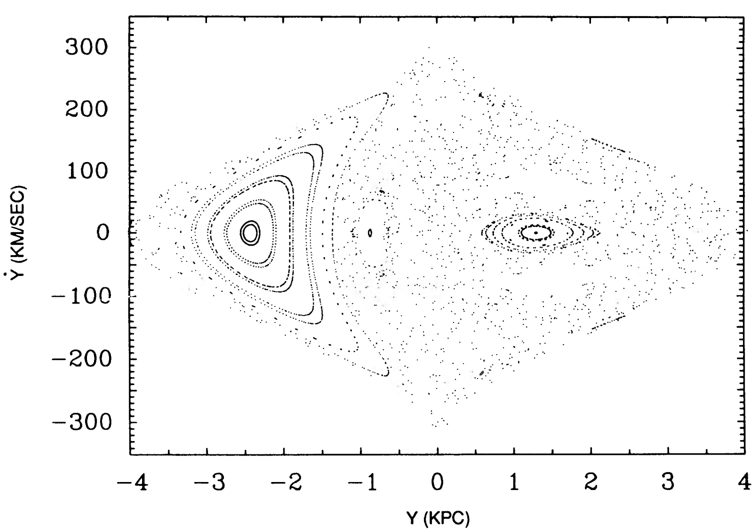

FIG. 7*c*

FIG. 7.—Surface of section plots for a rapidly rotating bar with black hole mass $M_{bh}/M_T = 0.03$, Jacobi constant corresponding to the particle reaching a maximum distance of $0.45a$, and axis ratio (*a*) $b/a = 0.45$, (*b*) $b/a = 0.35$, and (*c*) $b/a = 0.25$.

TABLE 1

VARIATION OF ILR WITH BLACK HOLE MASS

M_{bh}/M_T	ILR_x	ILR_y
0.01.........	0.8	0.90
0.05.........	1.5	1.88
0.09.........	1.8	2.10
0.13.........	2.1	3.94
0.15.........	2.2	4.06
0.17.........	2.3	4.16

along the y-axis moves out from 0.9 kpc to 4.16 kpc as the mass of the black hole increases from 1% to 17% of the total mass. An increase in the outer ILR causes the region in phase space occupied by orbits of the B family to decrease (see Contopoulos and Papayannopoulos 1980). For a black hole mass of 15% the outer ILR along the y-axis reaches 4.06 kpc which is the edge of the bar along this axis. The volume in phase space occupied by B orbits has gone down to $\sim 2\%$ for this case (Fig. 5). When the outer ILR moves outside the bar all B orbits are destroyed.

b) Variation of Bar Axial Ratio (b/a)

The effect of a black hole of mass 0.03 M_T was examined for three bars with $b/a = 0.45$, 0.35, and 0.25 and all other parameters held constant. In each case $R_{cr}/a = 1$, and the Jacobi constant was fixed so that the star could go to a maximum distance of 0.45a. The surface of section for the three cases is shown in Figure 7. There does not appear to be a major change in the structure of the surface of section as b/a decreases from 0.45 to 0.35. However, when the bar axial ratio is reduced to 0.25 most of the outer invariant curves dissolve because the orbits they represent have become stochastic. Only a very small region of the surface of section is now occupied by regular orbits. An examination of the variation of the phase

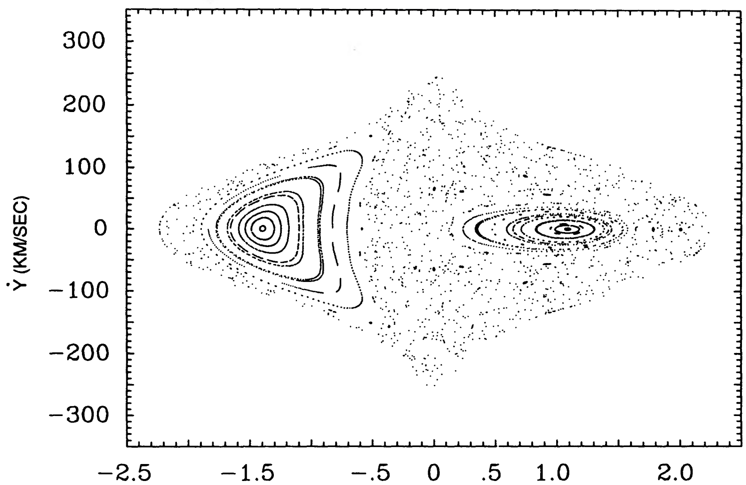

FIG. 8a

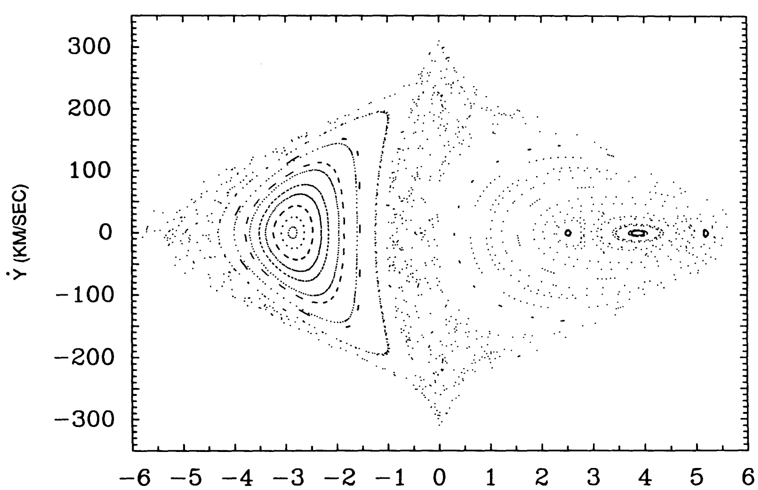

FIG. 8b

FIG. 8.—Surface of section plots for a rapidly rotating bar with black hole mass $M_{bh}/M_T = 0.03$, $b/a = 0.45$, and Jacobi constant corresponding to the particle reaching a maximum distance of (a) 0.25a and (b) 0.65a.

space volume ratio, P, with the bar axial ratio (Fig. 5) shows that while P varies slowly from $\sim 44\%$ to $\sim 41\%$ as b/a decreases from 0.45 to 0.35, the effect is much more dramatic for $b/a = 0.25$ when P goes down to $\sim 3\%$. In each case a computation was done for a bar without a black hole, and it was found that $P \sim 48\%$ in all cases. It seems quite clear that a very small black hole will destroy a thin bar, while a thicker bar is far more robust to black holes.

c) *Variation of Jacobi Constant*

A black hole of mass $0.03M_T$ causes greater ergodicity when the Jacobi constant corresponds to a maximum distance of $0.25a$ reached by the star than for distances $0.45a$ and $0.65a$. This is appparent both from the surface of section (Figs. 7*a* and 8) as well as from the variation of the phase space volume ratio (Fig. 5). The surface of section for stars with the largest energy considered here shows strong invariant curves with regions containing islands of higher order resonances. As the energy is decreased these islands disappear, but the volume in phase space occupied by B orbits increases slightly from $\sim 38\%$ in the previous case to $\sim 44\%$. Decreasing the energy further causes the outermost orbits to become stochastic and only $\sim 9\%$ of the phase space contains regular orbits. Thus the orbits of stars which do not have enough energy to go far from the black hole become stochastic more readily than those of stars with higher energy.

IV. SUMMARY

In summary, a black hole or central mass concentration in a barred galaxy can act to dissolve a bar. The fundamental orbits (called B orbits) supporting the bar are the orbits elongated in the direction of the bar. As the black hole mass increases, an ILR appears and moves outward. The B orbits disappear when the ILR reaches the end of the bar. This effect is significantly increased if the bar is thinner. Orbits that stay closer to the central mass with smaller Jacobi constants become stochastic more easily.

It is well known that ergodicity sets in when neighboring resonances overlap (see Ford 1978). It seems intuitively apparent that in the cases studied in this paper the resonance overlap between the forced family of B orbits and the natural family of A orbits anti-aligned with the bar accounts for the stochastic behavior of the orbits within the ILR. No attempt has been made here to examine this theory and it remains an obvious candidate for future research.

It is a pleasure to thank Daniel Pfenniger for many enlightening discussions of this work and for a careful reading of this manuscript. We also thank Andrew May and Peter Teuben for similarly enlightening discussions of the early part of this study. We also gained considerable stimulation from discussions at the Tucson workshop on Orbital Dynamics the meeting on Interacting Galaxies in Heidelberg in particular with James Binney, Ken Freeman, Ortwin Gerhard and Tim de Zeeuw.

REFERENCES

Athanassoula, E., Bienayme, O., Martinet, L., and Pfenniger, D. 1983, *Astr. Ap.*, **127**, 349.
Binney, J., Gerhard, O. E., and Hut, P. 1985, *M.N.R.A.S.*, **215**, 59.
Binney, J., and Tremaine, S. 1987, *Galactic Dynamics* (Princeton: Princeton University Press).
Chandrasekhar, S. 1969, *Ellipsoidal Figures of Equilibrium* (New Haven: Yale University Press).
Contopoulos, G., and Papayannopoulos, Th. 1980, *Astr. Ap.*, **92**, 33.
De Boor, C. 1978, *A Practical Guide to Splines* (New York: Springer-Verlag).
de Vaucouleurs, G., and Freeman, K. C. 1972, *Vistas Astr.*, **14**, p. 163.
De Zeeuw, T., and Merritt, D. 1983, *Ap. J.*, **267**, 571.
Dressler, A. 1988, *Ap. J.*, **234**, 701.
Fehlberg, E. 1969, *Computing*, **4**, 93 (in German).
———. 1970, *Computing*, **5**, 184 (in German).
Ford, J., 1978 in *AIP Conf. Proc. 46, Topics in Nonlinear Dynamics. A Tribute to Sir Edward Bullard*, ed. S. Jorna (New York: AIP), p. 121.
Franx, M., and Illingworth, G. 1988, *Ap. J. (Letters)*, **327**, L55.
Gerhard, O. E., Binney, J. 1985, *M.N.R.A.S.*, **216**, 467.
Jedrzejewski, R., and Schechter, P. L. 1989, *Astr. J.*, **98**, 147.
Kormendy, J. 1988, *Ap. J.*, **325**, 40.
Lake, G., and Norman, C. 1983, *Ap. J.*, **270**, 51.
Miralda-Escude, J., and Schwarzschild, M. 1989, *Ap. J.*, **339**, 752.
Norman, C. A., May, A., and van Albada, T. S. 1985, *Ap. J.*, **296**, 20.
Patterson, T. N. L. 1968*a*, *Math. Comput.*, **22**, 347.
———. 1968*b*, *Math. Comput.*, **22**, 877.
Perek, L. 1962, *Adv. Astr. Ap.*, **1**, 165.
Pfenniger, D., and de Zeeuw, T. 1989, in *Dynamics of Dense Stellar Systems*, ed. D. Merrit (Cambridge: Cambridge University Press.)
Pfenniger, D. 1990, *Astr. Ap.*, **230**, 55.
Rees, M. J. 1984, *Ann. Rev. Astr. Ap.*, **22**, 471.
Richstone, D., and Dressler, A. 1988, *Ap. J.*, **324**, 701.
Sargent, W. L. W., Young, P. J., Boksenberg, A., Shortridge, K., Lynds, C. R., and Hartwick, D. 1978, *Ap. J.*, **221**, 731.
Scoville, N. Z., Sanders, D. B., Sargent, A. I., Soifer, B. J., Scott, S. C., and Lo, K. Y. 1986, *Ap. J. (Letters)*, **311**, L47.
Teuben, P. J., and Sanders, R. H. 1985, *M.N.R.A.S.*, **212**, 257.
Tonry, P. J. 1987, *Ap. J.*, **322**, 932.
Udry, S., and Pfenniger, D. 1988, *Astr. Ap.*, **198**, 135.
Van Albada, T. S., and Sanders, R. H. 1982, *M.N.R.A.S.*, **201**, 303.

HASHIMA HASAN and COLIN NORMAN: Space Telescope Science Institute, 3700 San Martin Drive, Baltimore, MD 21218